frontiers | Frontiers in Environmental Science

TYPE Original Research
PUBLISHED 03 October 2022
DOI 10.3389/fenvs.2022.945192

OPEN ACCESS

EDITED BY
Tao Zhang,
China Agricultural University, China

REVIEWED BY
Fang Li,
Donghua University, China
Chamindra L. Vithana,
Southern Cross University, Australia

*CORRESPONDENCE
Kun Bai,
baikun@hfuu.edu.cn

SPECIALTY SECTION
This article was submitted to Water and Wastewater Management, a section of the journal Frontiers in Environmental Science

RECEIVED 16 May 2022
ACCEPTED 05 August 2022
PUBLISHED 03 October 2022

CITATION
Bai K, Liu W, Zhao M, Li K and Tian Y (2022), Numerical simulation study of oil–water separation based on a super-hydrophilic copper net.
Front. Environ. Sci. 10:945192.
doi: 10.3389/fenvs.2022.945192

Numerical simulation study of oil–water separation based on a super-hydrophilic copper net

Kun Bai*, Weinan Liu, Maoyu Zhao, Kaifang Li and Yiming Tian

School of Advanced Manufacturing Engineering, Hefei University, Hefei, China

Green and environmentally friendly oil–water separation is an important technique for reducing environmental pollution. In this study, the oil–water separation effect of the super-hydrophilic copper net was optimized through numerical simulation and orthogonal experiments. To be specific, a super-hydrophilic copper net was prepared using the solution etching method to perform oil–water separation experiments, and a favorable oil–water separation effect was achieved. First, the influences of oil–water flow velocity, copper net mesh size, and surface wettability on the oil–water separation effect of the super-hydrophilic copper net were explored via single-factor experiments. The results showed that the oil resistance of the super-hydrophilic copper net degraded, and its oil–water separation effect became poor due to the increasing oil–water flow velocity, enlarged copper net mesh size, and reduced oil contact angle on the surface of the super-hydrophilic copper net. On this basis, the optimized oil–water separation parameters were obtained through orthogonal experiments. The optimized process parameters were as follows: velocity = 0.1 m/s, copper net mesh size = 30 μm, oil contact angle = 150°, and oil removal rate = 95.7%. Furthermore, the copper net was etched using sodium hydroxide and sodium persulfate mixed solution to prepare a 500-mesh super-hydrophilic copper net for the oil–water separation experiment and then the oil removal rate reached 96.4%. The study results provide a theoretical basis, method, and means for the practical application of super-hydrophilic copper nets.

KEYWORDS

super-hydrophilic, copper net, oil–water separation, numerical simulation, contact angle

1 Introduction

With economic development, oily wastewater discharge and treatment difficulties are continuously aggravated. The economical and efficient treatment of oily wastewater can not only save resources and promote resource recycling but also be conducive to environmental protection (Zhang and Zhang, 2018; Chen, 2019; Lu et al., 2020).

Oily wastewater mainly comes from the petroleum industry and food processing industry (Song and Wang, 2011; Yu, 2015; Hu et al., 2021; Xu, 2021; Liu et al., 2022). Oil–water separation technology mainly includes gravity separation, centrifugal separation, membrane

separation, electrolysis separation, and air flotation separation (Hu et al., 2015; Shao and Zhong, 2015; Zhang et al., 2017; Zhang et al., 2021). The membrane separation technology is more effective and less costly to operate, but it is prone to blockage when treating oily wastewater with a high oil content, resulting in membrane contamination. Superwetting materials are capable of rapid efficient oil–water separation by virtue of oil–water wettability difference, without secondary pollution, which has been deeply investigated by scholars. Zhang et al. (2018a) experimentally prepared a stainless steel net with super-hydrophobic and super-oleophilic characteristics to explore its oil–water separation ability and self-cleaning ability; Jung and Bhushan (2009) established a model and used to predict the oil drop contact angle in water by studying the wetting behaviors of water drops and soil in a three-phase interface; Zhang et al. (2018b) ablated the Al, Fe, Cu, Mo, and stainless steel surfaces using lasers and prepared rough micro-nanocomposite surfaces. With the inherently high surface energy, Al, Fe, Cu, Mo, and stainless steel surfaces all showed super-hydrophilic and underwear super-oleophobic properties. The previously mentioned scholars used the prepared super-wettable materials to separate oil and water and achieved excellent results. However, the actual oil–water separation environment is often harsh and superwetting materials do not give good oil–water separation results in practice. With further research, more and more results showed that when the superwetting material is impacted, the oil–water separation effect will be affected (Pi et al., 2017; Zhao et al., 2018). In recent years, computer simulation theories of fluid and material properties have been gradually developing. Liu and Yu, (2010) constructed a super-hydrophobic microchannel flow model and studied its flow characteristics via the numerical simulation technique; Qin (2013) explored the oil–water separation effect of a super-hydrophobic membrane-based spiral oil–water separator through the numerical simulation technique.

In this study, the flow field conditions on the water drop–oil drop contact surface of a super-hydrophilic copper net were simulated via FLUENT software. The influences of three factors—oil–water flow velocity, copper net mesh size, and oil contact angle—on oil–water separation were mainly studied. On this basis, the aforementioned influencing factors were subjected to an orthogonal experiment, and optimized process parameters were obtained. The super-hydrophilic copper net was prepared according to the process parameters, and oil–water separation experiments were conducted to verify the reasonableness of the simulation results.

2 Materials and methods

2.1 Procedure of the simulation study

2.1.1 Modeling

The wettability of materials is greatly influenced by their surface microstructure. Periodic rough surfaces, aperiodic rough surfaces, and composite rough surfaces can be prepared through laser ablation and chemical etching (Pan et al., 2010; Cui et al., 2017). In this study, the surface microstructure of the super-hydrophilic copper net was simplified into a periodically distributed groove to simplify the calculation, and a 2D structure of its cross section was taken to establish a 2D model through Gambit software, as shown in Figure 1.

FIGURE 1
Schematic diagram of the groove structure for the super-hydrophilic copper net.

When simulating the oil–water separation of the super-hydrophilic copper net, the influences of three factors—velocity, net mesh size, and oil contact angle on the copper net surface—on the oil–water separation effect were mainly explored. The volume of fluent model (VOF model) (Feng and Yao, 2012; Zhang and Yan, 2013) can be used to acquire clear interfaces between different phases by setting their surface tension and wall surface contact angle. Hence, the VOF model was chosen to simulate the oil–water separation of this super-hydrophilic copper net by abiding by the conservation law of mass, momentum, and energy, with the basic governing equation as follows:

The continuity equation of the VOF model is:

$$\frac{\partial \rho}{\partial t} + \nabla(\rho v) = 0. \quad (1)$$

The continuity equation of the volume fraction is:

$$\frac{\partial \alpha_i}{\partial t} + v\nabla(\alpha_i) = 0. \quad (2)$$

The momentum conservation equation is:

$$\frac{\partial(\rho v)}{\partial t} + \nabla(\rho v v) = -\nabla P + \nabla\left[\mu\left(\nabla v + \nabla v^T\right)\right] + \rho g + F, \quad (3)$$

where ρ is the density, kg/m^3; v denotes the velocity vector, m/s; t represents time, s; ∇ is a mathematical operator notation; α_i is the volume fraction of phase i ; is the dynamic viscosity of fluid; g is the gravitational acceleration, m/s^2; P is the pressure intensity, Pa; and F represents the equivalent body force form of surface tension, N.

2.1.2 Numerical calculation method and boundary conditions

In this study, the flow field condition on the oil drop–water drop contact surface of a super-hydrophilic copper net was simulated. To simplify the calculation, a laminar flow model was selected. Given that a transient problem was the simulation object, pressure-implicit with the splitting of operators (PISO) algorithm was selected to accelerate the convergence rate of single iterative steps during

TABLE 1 Experimental reagents and substrates.

Reagent	Specification
$Na_2S_2O_8$	Analytically pure
Na(OH)	Analytically pure
C_2H_6O	Analytically pure
H_2O	-
Cu	500-mesh

transient calculation, harvesting a good convergence effect. As for the selection of the discretization method, the body force weighted scheme was chosen for pressure, second-order upwind discretization format for momentum, and geometric reconstruction format for the volume fraction. The initialization value of the sub-relaxation factor was set to default.

In this simulation, gravitational acceleration was set at 9.8 m/s^2, initial operating pressure at 101,325 Pa, and water contact angle at 0°. Three-phase (oil, water, and air) fluids were involved in the simulation of oil–water separation for a super-hydrophilic copper net. To clearly observe the flow field conditions on the oil drop–water drop contact surface of this super-hydrophilic copper net, the three-phase computational domains were divided through patch function, where air was set as the primary phase, and the volume fractions of all the three phases in their respective computational domains were set at 1. The tensions on oil and water surfaces were set at 0.029 and 0.072 N/m, respectively.

2.1.3 Range analysis

Range analysis was performed according to the orthogonal experimental results. The experimental results corresponding to the m level of factors in column j as well as K_{jm} and its mean value $_{jm}$ were calculated. Moreover, the range R_j of factors in column j was calculated based on the $_{jm}$ value:

$$\eta = \frac{C_1 - C_2}{C_1} \quad (4)$$

Here, R reflects the variation range of experimental results in case of changes in the factors in column j. A greater R-value manifested a greater influence of this factor on experimental indexes, so the sequence of influencing factors could be judged according to R.

2.2 Procedure of Cu net mesh and oil–water separation

The reagents required for the preparation of the super-hydrophilic copper net and super-hydrophobic copper net experiments are shown in Table 1.

FIGURE 2
Surface contact angle of the super-hydrophilic copper net.

A 500-mesh red copper net with a mesh size of 30 μm was selected as the substrate, and an etching solution was prepared by mixing 25 ml of 1 mol/L sodium hydroxide solution and 25 ml of 0.15 mol/L $Na_2S_2O_8$ solution. The dried red copper net was placed in the etching solution for reaction at room temperature for 60 min and then taken out and washed using deionized water. Subsequently, it was dried up in a blast air oven to prepare a super-hydrophilic copper net. The hydrophilicity of the super-hydrophilic copper net was examined using the OCA15EC optical contact angle meter and SU8010 scanning electron microscope, and the testing process was as follows: when measuring the contact angle of the prepared copper net surface, the SNS syringe needle was selected, and the dosing volume was set to 3 μL. The water was dropped at a dosing rate of 1 μL/s, and a thin film was formed on the surface of the copper net. The indirect contact angle was measured to be 0°, indicating that the copper net is super-hydrophilic, as shown in Figure 2.

The copper net was cut into 10 mm × 10 mm specimens, and the surface morphology of the prepared copper net was characterized using a cold field emission scanning electron microscope electron gun at an acceleration voltage of 15 KV. The surface morphologies of this super-hydrophobic copper net were characterized as shown in Figure 3. After etching through the mixed solution, many tiny clusters attached on the copper net matrix and presented ordered growth around. It could be observed that micrometer needle-like structures were generated on the surface of the copper net substrate, which was mutually crossed and grew around in an unordered way. These clusters and micrometer needle-like structures formed composite micro-nanostructures on the copper net surface, thus greatly increasing the roughness of the copper net surface and endowing it with super-hydrophilicity.

To test the oil–water separation effect of this 500-mesh super-hydrophilic copper net, an oil–water separation device was designed

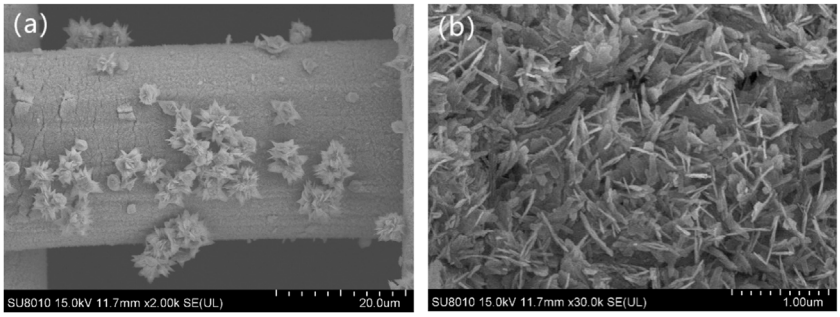

FIGURE 3
Surface morphologies of the super-hydrophilic copper net.

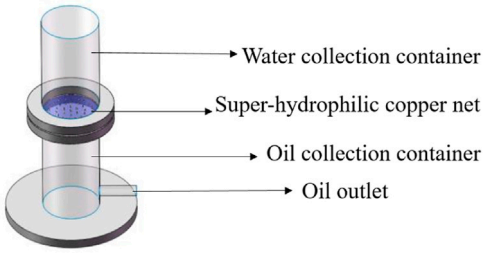

FIGURE 4
Schematic diagram of the oil–water separation device.

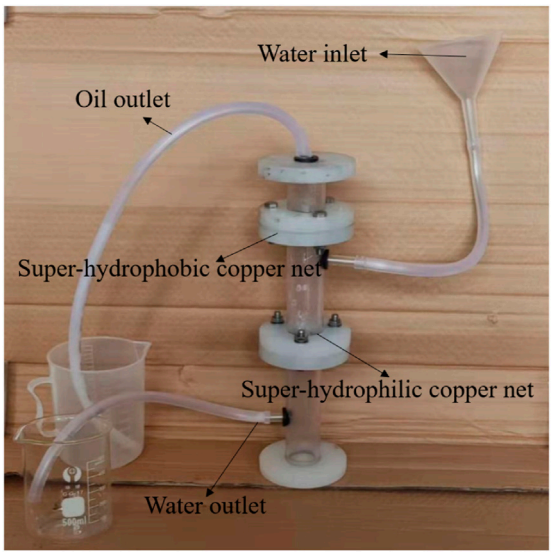

FIGURE 5
Experimental separation device.

as shown in Figures 4, 5. Using restaurant oily wastewater as the separation object, it was first treated by air flotation and the measured animal and vegetable oil content was 54.5 mg/L, and the oil content was still high. Then, the secondary treatment of this oily wastewater was carried out by using a super-hydrophilic copper net. Before the oil–water separation experiment, the super-hydrophilic copper net was fully wetted using water. Next, 500 ml of oily restaurant wastewater pretreated through air flotation was taken and made to flow into the vessel slowly along the inner wall to prevent the oil–water separation effect from being impacted by too high oil–water flow velocity.

3 Results and discussion

3.1 Calculated results and analysis of the simulation study

3.1.1 Oil–water flow velocity

The flow field conditions when oil and water drops contacted the super-hydrophilic copper net were simulated at simulation velocities of 0.1, 0.5, and 1 m/s under the net mesh size of 10 μm and oil contact angle of 150°. At the left was the aqueous phase and at the right was the oil phase, as shown in the following Figure 6.

It could be known from Figure 6 that water drops could completely wet and penetrate through this super-hydrophilic copper net. At a velocity of 0.1 m/s, oil drops failed to wet the super-hydrophilic copper net and were intercepted above it, thus realizing the goal of efficient oil–water separation. As the velocity was elevated to 0.5 m/s, the dynamic pressure was elevated, and oil drops were forcibly extruded into the groove structure on the partial copper net surface, but they did not completely wet the copper net, which was still oleophobic to some extent. When the velocity was increased to 1 m/s, oil drops were forcibly extruded into the groove structure on the copper net surface and passed

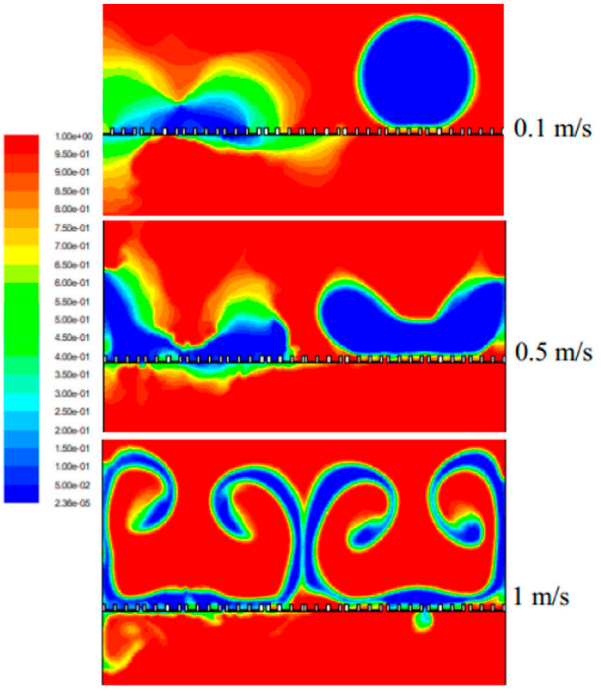

FIGURE 6
Cloud picture of the oil–water volume fraction at a velocity of 0.1, 0.5, and 1 m/s.

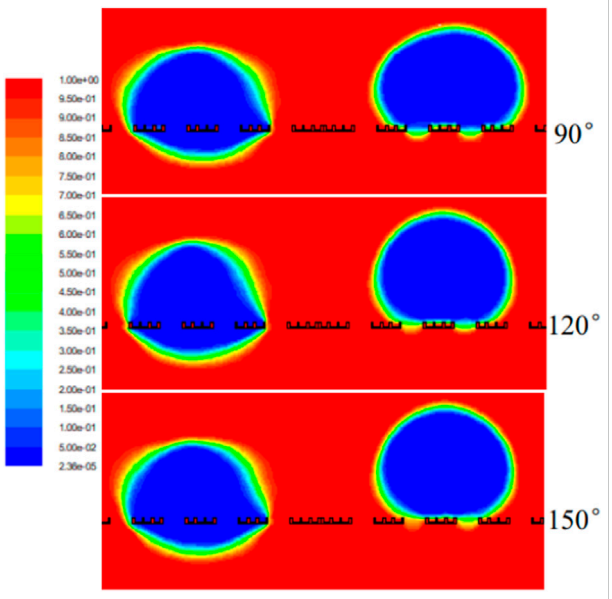

FIGURE 8
Cloud picture of the oil–water volume fraction under the oil contact angle of 90°, 120°, and 150°.

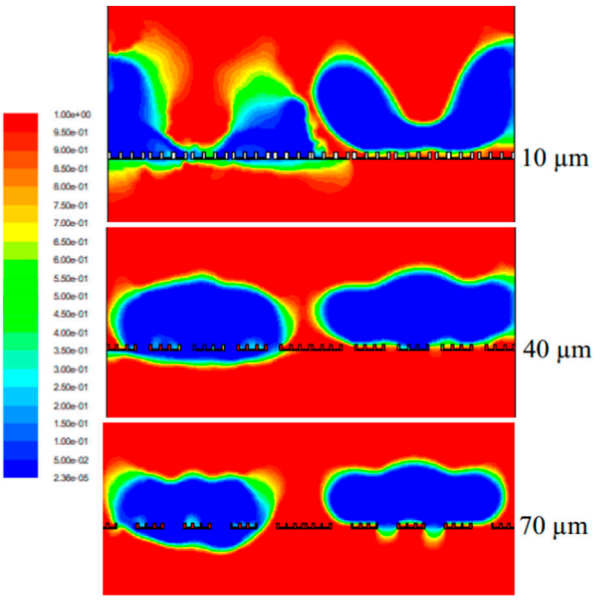

FIGURE 7
Cloud picture of the oil–water volume fraction under the copper net mesh size of 10, 40, and 70 μm.

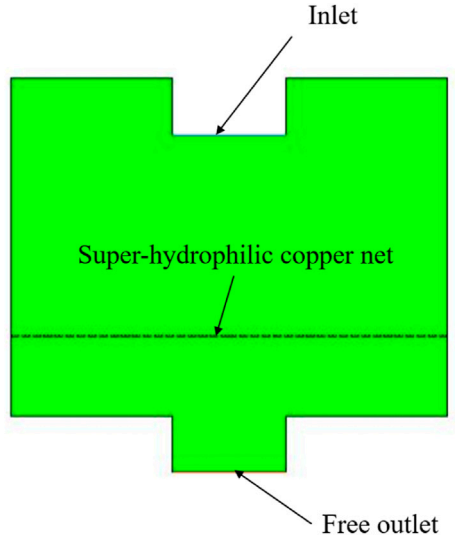

FIGURE 9
2D model drawing of the super-hydrophilic copper mesh.

TABLE 2 Factor levels in the orthogonal experiment.

Level	Copper net mesh size (μm)	Velocity (m/s)	Oil contact angle (°)
1	100	0.1	90
2	70	0.5	120
3	30	1	150

TABLE 3 Orthogonal experiment and results.

No.	Copper net mesh size (μm)	Velocity (m/s)	Oil contact angle (°)	Oil removal rate (%)
1	100	0.1	90	28.3
2	100	0.5	120	24.6
3	100	1	150	35.3
4	70	0.5	150	43.2
5	70	0.1	120	64.7
6	70	1	90	10.1
7	30	0.5	90	26.7
8	30	1	120	31.6
9	30	0.1	150	95.7

through the net via meshes, and this super-hydrophilic copper net could not realize efficient oil–water separation under this circumstance.

3.1.2 Copper net mesh size

The flow field conditions when oil and water drops contacted the super-hydrophilic copper net were simulated at the velocity of 0.5 m/s under the oil contact angle of 150° and the copper net mesh size of 10, 40, and 70 μm, respectively, as shown in the following Figure 7.

It could be known from Figure 7 that the copper net mesh size had a bearing on its oleophobic properties. When the copper net mesh size was continuously enlarged, oil drops would finally pass through this super-hydrophilic copper net. As the copper net mesh size gradually increases, the area of the super-hydrophilic copper mesh also increases, and its impact resistance will be weakened, so the effect of oil–water separation will become worse. Hence, it is important to select an appropriate copper net mesh size in order to enhance the oil–water separation effect.

3.1.3 Contact angle

The flow field conditions when oil and water drops contacted the super-hydrophilic copper net were simulated at the velocity of 0.1 m/s under a copper net mesh size of 70 μm and oil contact angles of 90°, 120°, and 150°, respectively, as shown in the following Figure 8.

As shown in Figure 8, at the velocity of 0.1 m/s and copper net mesh size of 70 μm, water drops could freely pass through the super-hydrophilic copper net at contact angles of 90°, 120°, and 150°. As the oil contact angle was gradually enlarged, the contact area between oil drops and super-hydrophilic copper net was smaller. At the oil contact angle of 90°, partial oil drops penetrated through this super-hydrophilic copper net. When the oil contact angle increased to 150°, oil drops were nearly completely obstructed above the super-hydrophilic copper net, with its oleophobic properties gradually enhanced, which was better for improving the oil–water separation effect.

3.1.4 Three-factor three-level orthogonal experimental analysis

The aforementioned simulation results revealed that velocity, net mesh size, and oil contact angle exerted important influences on the oil–water separation effect of this super-hydrophilic copper net. Based on the simplified 2D super-hydrophilic copper net surface structure, a 2D numerical simulation model of this super-hydrophilic copper net was constructed (Figure 9). Then, a three-factor three-level orthogonal experiment was carried out to further explore the influencing degrees of velocity, copper net mesh size, and contact angle on the oil–water separation effect of the super-hydrophilic copper net. The factor levels in the orthogonal experiment are listed in Table 2, and the orthogonal experiment and its results are presented in Table 3.

TABLE 4 Range analysis of orthogonal experimental results.

Index	Level	Copper net mesh size (μm)	Velocity (m/s)	Oil contact angle (°)
	1	88.2	188.7	65.1
	2	118	94.5	120.9
	3	154	77	174.2
	1	29.4	62.9	21.7
	2	39.3	31.5	40.3
	3	51.3	25.7	58.1
Optimal level		3	1	3
		21.9	37.2	36.4
Sequence	Velocity > oil contact angle > copper net mesh size			

During numerical simulation, outlet flow monitoring was set in FLUENT software. A stable outlet flow indicated that the oil–water separating flow field of this super-hydrophilic copper net was stable. In this case, the mass flow data of inlet and outlet oil were, respectively, recorded, and the oil removal rate was calculated accordingly through the following formula:

$$R_j = \max(K_{j1}, K_{j2}, \ldots K_{jm}) - \min(K_{j1}, K_{j2}, \ldots K_{jm}) \quad (5)$$

where η oil removal rate;

C1 mass flow of inlet oil, kg/s; and

C2 mass flow of outlet oil, kg/s.

The range analysis of orthogonal experimental results is presented in Table 4. It could be known from the range analysis that the sequence of factors influencing the oil removal effect of this super-hydrophilic copper net was as follows: oil–water flow velocity > oil contact angle > copper net mesh size. The orthogonal experimental results reflected that the oil removal rate reached the highest value (95.7%) at the velocity of 0.1 m/s, oil contact angle of 150°, and copper net mesh size of 30 μm. Figure 10 is drawn under the aforementioned process parameters. As shown in Figure 10, oil was basically intercepted above the super-hydrophilic copper net, while only a small quantity of oil passed through this net, which showed good oil resistance and water drainage functions under this circumstance.

3.2 Results of the oil–water separation experiment using the newly synthesized Cu net mesh

The animal and vegetable oil concentrations in water before and after the experiment were measured using an infrared oil meter

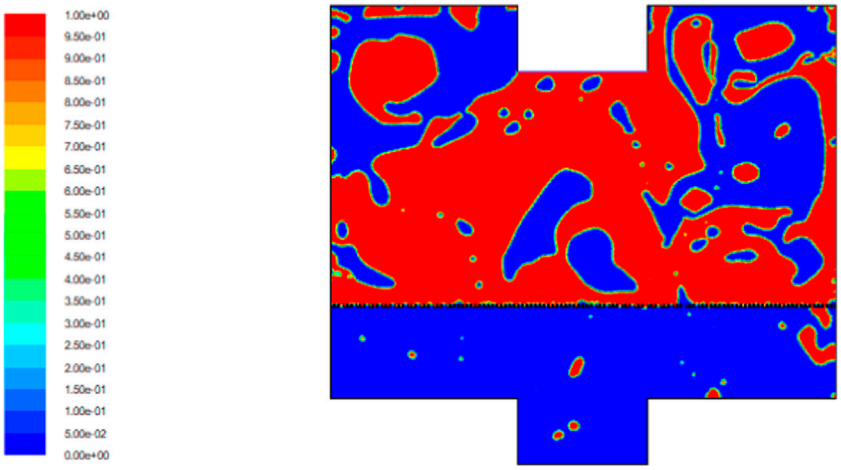

FIGURE 10
Cloud picture of the oil-phase volume fraction.

TABLE 5 Results of the oil–water separation experiment.

Water sample before the experiment (mg/L)	Water sample after the experiment (mg/L)	Oil removal rate (%)
54.5	1.98	96.4

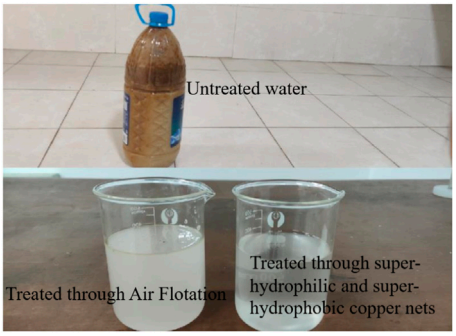

FIGURE 11
Comparison diagram of water qualities before and after treatment.

(Table 5). Through the treatment using a 500-mesh super-hydrophilic copper net, a good oil removal effect was achieved at a reasonable oil–water flow velocity, and the content of animal and vegetable oils was reduced to 1.98 mg/L, with the oil removal rate reaching 96.4%, which was approximate to the numerical simulation result. The water qualities before and after the treatment were compared as shown in Figure 11.

The oil removal rates mentioned in Sun et al. (2018) were 98.8, 98.75, 99, 99.5, and 99.95%. Further experiments were conducted with three such oil–water separation devices connected in series, and it was measured that the content of animal and vegetable oils was reduced to 0.34 mg/L, and the oil removal rate could reach 99.4%, which is better or close to several membrane separation techniques mentioned in the reference (Sun et al., 2018).

4 Conclusion

In this study, the surface structure of the super-hydrophilic copper net was simplified and three single-factor simulation experiments of oil–water flow rate, copper mesh pore size, and oil contact angle were conducted separately using FLUENT software. The simulation results show that all three factors have an important effect on the oil–water separation effect of the super-hydrophilic copper net. On this basis, the process parameters of oil–water separation using the super-hydrophilic copper net were optimized by orthogonal tests. The super hydrophilic copper net was prepared by etching the copper mesh with a mixture of sodium hydroxide and sodium persulfate, and the oil–water separation experiment was conducted, and then a better oil–water separation effect was obtained. The main conclusions are as follows:

1) With the increase in the oil–water flow velocity and copper net mesh size and the reduction of the oil contact angle on the surface of this super-hydrophilic copper net, its oil resistance performance is degraded, thus failing to achieve efficient oil–water separation.
2) The range analysis of orthogonal experimental results reveals that the oil–water flow velocity has the greatest influence on the oil–water separation effect, followed by the oil contact angle and the copper net mesh size. The optimized process parameters were as follows: velocity was 0.1 m/s, copper net mesh size was 30 μm, oil contact angle was 150°, and oil removal rate reached 95.7%.
3) Through the oil–water separation experiment through 500-mesh super-hydrophilic and super-hydrophobic copper nets, the oil removal rate reached 96.4%, being approximate to the numerical simulation result. Therefore, the reasonability and feasibility of the simulation experiment were further proved.
4) The oil removal rate can reach 99.4% by connecting three super-hydrophilic copper net oil–water separation devices in series. This technology has a high oil removal rate and a simpler method of membrane material preparation.

Data availability statement

The original contributions presented in the study are included in the article/Supplementary Material; further inquiries can be directed to the corresponding author.

Author contributions

Conceptualization, KB and WL; methodology, KB, WL, and MZ; software, KB and WL; validation, WL and KL; formal analysis, KB and WL; investigation, KB, MZ, and KL; resources, KB and WL; writing—original draft preparation, KB; writing—review and editing, WL and YT; supervision, KB, WL, and MZ; and project administration,

KB. All authors have read and agreed to the published version of the manuscript.

Conflict of interest

The authors declare that the research was conducted in the absence of any commercial or financial relationships that could be construed as a potential conflict of interest.

Publisher's note

References

Chen, Y. M. (2019). Review of treatment of oily wastewater by combined process. *Ningxia Eng. Technol.* 18 (03), 271–274. [in Chinese]. doi:10.1016/j.arabjc.2013.07.020

Cui, Q. Z., Li, C. X., and Ye, X. M. (2017). Effect of structural parameters on the turbulent resistance characteristics of superhydrophobic microchannels. *Electr. Power Sci. Eng.* 33 (07), 52–57. [in Chinese]. doi:10.1063/5.0056952

Feng, L., and Yao, Q. Y. (2012). Numerical simulation of gas-liquid two-phase flow based on the VOF model in pump station pressure piping. *China Rural Water Hydropower* (12), 124–126+130. [in Chinese].

Hu, H., Wang, F., He, W. Z., and Li, G. M. (2015). Research on oil separation from catering swill by microwave and centrifugation. *Environ. Eng.* 33 (10), 77–80+125. doi:10.13205/j.hjgc.201510017

Hu, T. Y., Tang, J., and Chen, Z. L. (2021). Progress of oily wastewater treatment in petroleum industry. *Technol. Water Treat.* 47 (06), 12–17. doi:10.1016/j.arabjc.2013.07.020

Jung, Y. C., and Bhushan, B. (2009). Wetting behavior of waterand oil droplets in three-phase interfaces for hydropho-bicity/philicity and oleophobicity/philicity. *Langmuir* 25 (24), 14165–14173. doi:10.1021/la901906h

Liu, Y., Sun, Y., Sun, Y. X., Guo, J., Liang, P., Xu, B. W., et al. (2022). Mechanism and experiment of micro-channel filtration by heterostructure media particles for oily wastewater treatment. *Chin. J. Environ. Eng.* 16 (02), 506–514. doi:10.12030/j.cjee.20210108

Liu, Z., and Yu, Z. J. (2010). Numerical simulation of water flow in the super-hydrophobic micro-tube. *Liaoning Chem. Ind.* 39 (9), 897–900. [in Chinese]. doi:10.3969/j.issn.1004-0935.2010.09.001

Lu, H., Liu, Y. Q., Dai, P. Y., Pan, Z. C., Li, Y. D., Wu, S. H., et al. (2020). Process intensification technologies for oil-water separation. *Chem. Industry Eng. Prog.* 39 (12), 4954–4962. [in Chinese]. doi:10.16085/j.issn.1000-6613.2020-0985

Pan, G., Huang, Q. G., Hu, H. B., and Liu, Z. Y. (2010). Wettability of superhydrophobic surface through tuning microcosmic structure. *Polym. Mater. Sci. Eng.* 26 (07), 163–166. [in Chinese].

Pi, P. H., Hou, K., Zhou, C. L., Li, D. G., Wen, X. F., Xu, S. P., et al. (2017). Superhydrophobic Cu2S@Cu2O film on copper surface fabricated by a facile chemical bath deposition method and its application in oil-water separation. *Appl. Surf. Sci.* 396, 566–573. doi:10.1016/j.apsusc.2016.10.198

Qin, J. X. (2013). *Design of spiral flow oil-water separator based on superhydrophobic membrane*. China: Southwest Petroleum University. [in Chinese].

Shao, Y. F., and Zhong, L. W. (2015). The improvement of oil-water separation technique based on gravitational sedimentation. *Telecom Power Technol.* 32 (06), 174–177+193. doi:10.1023/B:WATE.0000038874.85413.05

Song, H. T., and Wang, R. (2011). Analysis of water quality and survey on oily waste water from universities' canteen. *J. Hubei Univ. Sci. Ed.* 33 (03), 323–327. doi:10.3969/j.issn.1000-2375.2011.03.013

Sun, Y., Zhou, L., Bian, T., Tian, X. X., Ren, W. K., Lu, C., et al. (2018). Efficacy evaluation of two commercial modified-live virus vaccines against a novel recombinant type 2 porcine reproductive and respiratory syndrome virus. *Vet. Microbiol.* 45 (8), 176–182. [in Chinese]. doi:10.1016/j.vetmic.2018.02.016

Xu, K. P. (2021). Research status and prospect of oily wastewater treatment methods. *Chem. Enterp. Manag.* (24), 21–22. doi:10.3390/w11122517

Yu, Z. Q. (2015). *Pollution status and prevention countermeasures of oily waste water in catering trade*. china: China Environmental Protection Industry, 47–49.07

Zhang, D., Wang, G., Zhi, S., Xu, K., Zhu, L. J., Li, W. W., et al. (2018). Superhydrophilicity and underwater superoleophobicity TiO2/Al2O3 composite membrane with ultra low oil adhesion for highly efficient oil-in-water emulsions separation. *Appl. Surf. Sci.* 458 (15), 157–165. doi:10.1016/j.apsusc.2018.07.052

Zhang, G. J., and Yan, Y. J. (2013). Numerical simulation method of water-entry impact at low speed for a missile based on VOF model. *J. Air Force Eng. Univ. Nat. Sci. Ed.* 14 (06), 23–26. [in Chinese]. doi:10.1088/1742-6596/1507/10/102028

Zhang, J. X., Ma, Y. Y., Zhou, M., Zhang, X. X., and Wang, C. C. (2017). Advances in oil-water separation technologies. *Water Purif. Technol.* 36 (12), 50–54+61.

Zhang, L. L., Chen, Q., Yin, M. H., Zheng, S. X., and Yang, X. Q. (2021). Emulsified wastewater treatment using membrane separation technique: A review. *Appl. Chem. Ind.* 50 (10), 2791–2796. doi:10.1088/1742-6596/1507/10/102028

Zhang, R., and Zhang, F. (2018). Development of oily wastewater treatment technology. *Contemp. Chem. Ind.* 47 (08), 1695–1697+1701. doi:10.13840/j.cnki.cn21-1457/tq.2018.08.044

Zhang, Z. H., Wang, H. J., Liang, Y. H., Li, X. J., Ren, L. Q., Cui, Z. Q., et al. (2018). One step fabrication of robust superhydrophobic and supero leophilic surfaces with self-cleaning and oil/water separation function. *Sci. Rep.* 8 (1), 3869. doi:10.1038/s41598-018-22241-9

Zhao, Z. E., Sun, S. H., Hu, Y. M., and Zhu, Y. (2018). Research progress on durability and evaluation methods of superhydrophobic surface. *Adv. Material Chem.* 6 (3), 56–65. doi:10.12677/amc.2018.63007